ASSESSMENT OF FLANKING TRANSMISSIONS IN MEASUREMENTS OF SOUND TRANSMISSION LOSS OF MULTI-LAYER PANELS

Can Nerse[1] *and* Sebastian Oberst[2]
Centre for Audio, Acoustics and Vibration (CAAV), Faculty of Engineering and Information Technology, University of Technology Sydney, Ultimo NSW 2007, Australia
email: [1]*can.nerse@uts.edu.au*, [2]*sebastian.oberst@uts.edu.au*

Stephen Moore[3] *and* Ian MacGillivray[4]
Maritime Division, Defence Science and Technology Group, Department of Defence, Fishermans Bend VIC 3207, Australia
e-mail: [3]*stephen.moore15@dst.defence.gov.au*, [4]*ian.macgillivray@dst.defence.gov.au*

The sound transmission loss measurements of small-sized panels ideally require perfect sealing of the panel frame and a rigid construction of the filler wall that encloses the panels. In practice, suppression of flanking transmission is achieved by having a sufficient isolation between both the source and the receiver rooms and blocking the indirect transmission by installing additional elements on the surfaces of both rooms. At the outer edges of the panel, the frame is supported by acoustically reflective materials and insulations to reduce the energy propagating into the wall. The sound transmission loss of the panels can be improved by installing layers that contribute to additional or more efficient dissipation. These layers are installed in such a way that they are tightly bolted into the frame with a niche being introduced on sides to further secure the panel within the opening. However, for panels with alternating layers of solid and porous materials, or with acoustic cavities, the structural rigidity of the supporting frame and joints are the primary factors that cause the flanking transmission. In this study, we investigate the extent of this transmission, and identify the vibration transmission paths and assess their negligibility in measurement of the sound transmission loss of the multilayer panels. A source-path-receiver approach has been proposed for ranking the critical transmission paths for different panel configurations. For this purpose, a numerical framework has been developed to measure the acoustic response of the room and vibration response of the structural elements at operating conditions. A finite element model in COMSOL is set to validate the results and is compared with an in-house analytical solution which shows good agreements. Assessment of the vibration and acoustic signals at sub-structures reveals transmission paths that are significant for the performance evaluation of multilayer panels.
Keywords: Sound transmission loss, vibration transmission, wave propagation, diagnostics, transfer path analysis

1. Introduction

Sound transmission loss (STL) of finite panels and partitions has been studied for many decades [1–4]. Theoretical calculations are based on infinite panel theory including finite or infinite baffles, panel edge effects and boundary conditions. However, in practice five major factors influence the STL measurement: panel design and manufacture, depth of niche, size of the receiving room and the source room, panel mounting as well other boundary conditions with regards to the wall and the niche.

Changing the size and thickness of the panel shifts the critical frequency, which is defined as the lowest coincidence frequency where the trace wavelength of the acoustic wave matches that of the structural vibration in bending. By variation of the panel size, modal frequencies and effective panel impedance also changes. The diffuse field forced radiation efficiency increases with sample size, indicating that smaller panels will have a higher STL below the coincidence frequency [5,6]. At the coincidence region the panel radiates sound very efficiently indicating that the panel itself becomes the dominant radiator with edge effects being reduced and, in general, size effects becoming negligible [7].

In most experimental studies which involve sound insulation materials in small openings, the acoustic baffle (otherwise known as the filler wall) is commonly a material of high density which also consists of several partitions, such as dry concrete, gypsum wall and glass wool. The test panel can either be installed at the source or receiving room end, or at a niche depth with respect to the surface of the baffle. The STL of a single panel in a niche is smaller than that found for an infinite rigid baffle and the maximum difference in STL occurs when the panel is installed at the centre of the aperture [8,9]. Furthermore, location affects the STL due to the tunnelling effect [10]: If the depth of a niche is comparable to the acoustic wavelength it acts as a waveguide, altering the sound field on both sides of the panel. For off-resonant frequencies which lie below the coincidence frequency, response of the panel increases with increasing niche depth, and sound pressure in the receiving room increases due to the shielding of near-grazing angles by the niche. The combined effect contributes to STL reduction when compared to a panel within an infinite rigid baffle. At the resonant frequencies, the niche results in reduction of the panel velocity and sound pressure in the receiving room; thus, increasing the STL from the panel [8,11]. The dependence of STL on niche depth and panel location makes the comparison and validation across different laboratory results difficult [12]. It is recommended by [13,14] that a staggered niche could be introduced to eliminate some of these frequency-dependent behaviours. The niche on the source side should be wide enough to reduce the coupling between the niche modes at both sides of the panel at large wavelengths. However, it is also noted that a larger value of the niche may also increase the STL at higher frequencies, thus leading to an overestimation of STL [11].

In the low frequency range, STL is influenced by the modal behaviour of the chambers, the built-in niche, and the panel. The number of modes and the strength of coupling between the various modes also affect the STL [11]. The frequency around in which modal behaviour of the chamber transitions into diffuse behaviour is expressed by the Schroeder frequency which is a function of the dimensions of the source and the receiving rooms' dimensions, and their reverberation time [15]. Furthermore, the STL results are affected by both the panel mounting conditions and the boundary conditions, while the boundary conditions alone become increasingly important at higher frequencies still below the coincidence frequency [8]. The STL above the coincidence frequency is largely independent of the laboratory design and the mounting conditions [16]. Above the coincidence frequency, there is a power flow which extends from the edges of the panel into the baffle [16,17]; this is highly dependent on the panel to baffle connections. Due to stiffness and damping of the wall segment under consideration, vibrational energy originating from the panel and travelling into the wall dissipates; this becomes more significant for heavier-weight designs in turn contributing to a higher STL. Figure 1 illustrates the possible transmission paths between the rooms in a test facility, which stem as source from either the partition (D) or the flanks (F) and being transmitted to either the partition (d) or the flanks (f). In this notation, Dd refers to the direct transmission path, whereas Df indicates transmission from the partition into the

flanking construction from which the sound then radiates. Fd and Ff correspond then to the transmission paths that originate from the flanking constructions and radiate through direct and flanking constructions, respectively [18]. In general, flanking transmission constitutes a combination of Df, Fd and Ff. However, there are very few comprehensive studies exploring the relationship between Dd, Df, Fd and Ff.

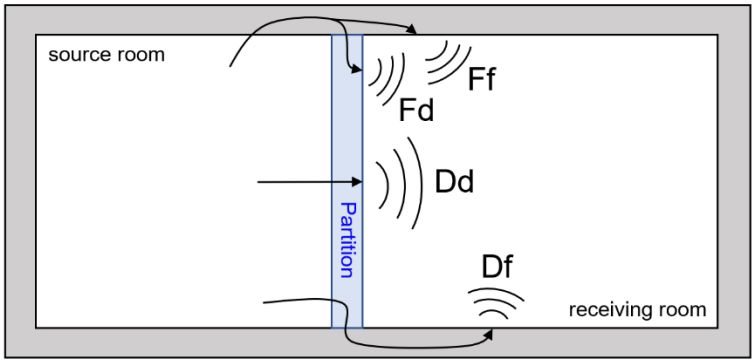

Figure 1: Schematic representation of the different transmission paths from source room to receiving room. Dd: direct transmission path from source room to receiving room through partition; Df: transmission path entering partition directly and radiating from flanking constructions; Fd: transmission path entering from flanking constructions and radiating from partition; Ff: transmission path entering and radiating from flanking constructions.

Hence, the main objective of this study is the STL measurement of finite panels of different material combinations in multi-layer configurations for the identification of direct and flanking transmission contributions in a simulated environment. For this purpose, a reliable and robust methodology has been developed to study the coupling mechanisms between different structural and acoustical domains by conducting accurate simulations in a validated prediction model created using a COMSOL 5.6 multiphysics software framework.

2. Modelling and Simulation Setup

Finite element analysis of the full model of the transmission loss suite is computationally expensive due to the extremely fine mesh requirements in high frequencies. A simplified model is developed to calculate the transmission loss by a reformulation of the original problem. The method in this study has an ideal diffuse field on the source side, and an ideal anechoic termination on the receiving side. The sound field on the source room is defined as a sum of uncorrelated plane waves of unit amplitude moving in random directions. Hence, the source room pressure field can be expressed as

$$p_{room} = \frac{1}{\sqrt{N}} \sum_{n=1}^{N} \exp\left(-i\left(k_{n,x} + k_{n,y} + k_{n,z}\right)\right) \exp\left(i\Phi_n\right) \tag{1}$$

where $k_{n,x} = \cos(\theta_n)$, $k_{n,y} = \sin(\theta_n)\cos(\psi_n)$, $k_{n,z} = \sin(\theta_n)\sin(\psi_n)$ and θ_n, ψ_n are polar angles while ϕ_n represents the phase. N is the number of plane waves and $i = \sqrt{-1}$. For each of the n in the summands in Eq. (1), a set of parameters for the incident plane wave direction is randomised. The summation is divided by $\sqrt{N}$ to ensure a constant acoustic intensity on the incident side.

For a test panel whose incident surface placed at $x = 0$, the reflected sound field is:

$$p_{refl} = \frac{1}{\sqrt{N}} \sum_{n=1}^{N} \exp\left(-i\left(-k_{n,x} + k_{n,y} + k_{n,z}\right)\right) \exp\left(i\Phi_n\right) \tag{2}$$

Then, the total pressure at the surface of the panel can be expressed as

$$p_{panel} = p_{room} + p_{refl} \tag{3}$$

The simulation model outlined herein is implemented in COMSOL Multiphysics (version 5.6), using the Structural Mechanics and Acoustics modules. By using an acoustic half-space, the diffuse field incident on the source side is implemented as a boundary load p_{panel} acting directly on the panel. The anechoic termination is achieved by a perfectly matched layer (PML) in an air medium, as shown in Fig. 2. Through this simplification Ff and Df flanking transmission paths (Fig. 1) were considered negligible, so only the radiated sound from the panel through direct and indirect transmission paths were calculated. The panel boundaries are fixed on the outer edges. Hence, the sound transmission loss is calculated by a ratio of incident (P_{in}) and transmitted power (P_{tr}) as follows,

$$\mathrm{STL} = 10\log_{10}(P_{in}/P_{tr}) \tag{4}$$

where $P_{in} = \mathrm{Re}(p_{room} \cdot v_{room})/4$ and $P_{tr} = SI_{tr}$; $(\cdot)$ is the dot operator and $v_{room} = (-\partial p_{room}/\partial x)/i\rho\omega$ is the acoustic particle velocity. S and I_{tr} are the panel surface area and transmitted intensity, respectively.

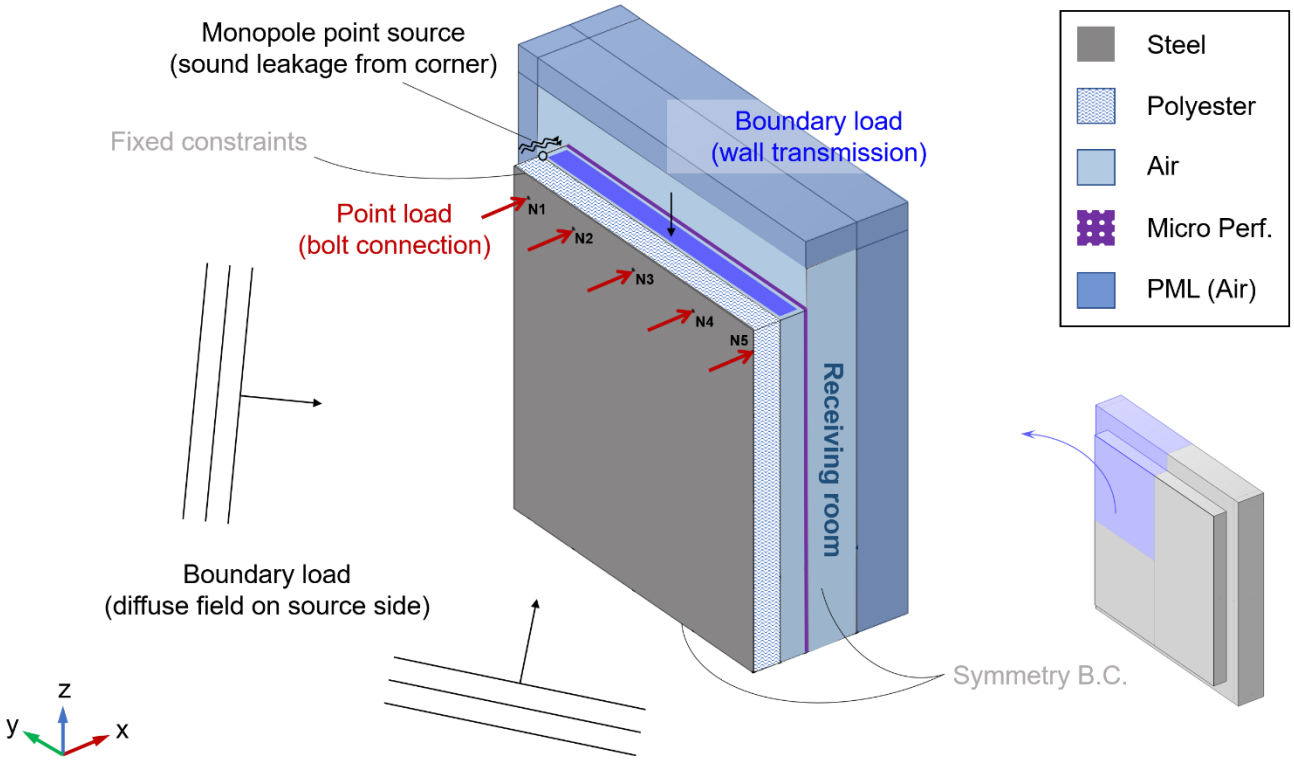

Figure 2: Visualisation of a multilayer panel in a quarter-section model of a reverberant–anechoic transmission loss measurement setting. The diffuse field on the reverberant (source) side is implemented as boundary load on the surface of the steel layer. The adjacent layers of the multilayer panel consist of polyester, air cavity, and a micro-perforated facing on the receiving room side. The locations for the point load (N1 to N5) and monopole source, which are approximations of bolt connection and sound leakage from corner, respectively, are shown for reference. The boundary load applied on the air cavity within panel construction denotes the flanking transmission from the surrounding wall into the panel.

The multi-layer panel of surface area 1×1 m^2 has a steel layer mounted on its source side. Fibrous insulation (polyester) with 50 mm thickness is installed adjacently, then on the receiving side a 0.3 mm thick microperforated facing with perforations of 0.5 mm diameter is installed, which is sepa-

rated from the fibrous insulation by a 50 mm air cavity, as shown in Fig. 2 (quarter-section model). The fibrous insulation and microperforated facing induce losses via friction and thermoviscous interactions at the micro-pores, respectively. In the numerical model, these losses are implemented in Poroacoustics module with flow resistivity, porosity, thermal/viscous characteristic lengths and tortuosity factor of the porous physical domain. The polyester material is characterised by its flow resistivity which is implemented in COMSOL by the Delany-Bazley-Miki poroelastic model [19]. The modelling of a microperforated panel can be computationally expensive due to dense mesh requirements in and between the holes. It has been shown that a thin, porous material can be expressed as an equivalent microperforated layer by using the geometrical parameters to estimate the corresponding porous material model [20]. Thus, only the pore parameters are calculated for the air medium. Table 1 summarises the material properties and dimensions for this multi material multi-layer panel configuration.

To discretise the solid and acoustic physical domains a mapped and sweep mesh algorithm is used. The former uses quadratic serendipity elements, while the latter employs quadratic Lagrange elements, which have a higher degree of freedom and more accurate in their u/p (displacement/pressure) formulation. The maximum and minimum element sizes in the acoustic domain are chosen with respect to frequency bandwidth, i.e., $c/5f_{max}$ and $c/20f_{max}$, respectively. The solid domain was discretised by at least 20 elements per wavelength of the of the eigenfrequencies of the bending modes. In the normal direction at the PML region, the mesh is discretised by 8 elements.

Table 1. Summary of the dimensions and material properties of the multi-layer panel used in the simulations. Here ρ, E, ν, η refer to the density, the elastic modulus, the Poisson's ratio and the structural loss factor, respectively. σ is the flow resistivity of the polyester material, and c is the speed of sound of the medium air, while d and p denote the diameter of the perforations and perforation ratio on the microperforated facing, respectively.

Material	Thickness t / Depth D	Properties
Steel	2.5 mm	$\rho_s = 7850\ \mathrm{kg/m^3}$ $E = 210\ \mathrm{GPa}$ $\nu = 0.3$ $\eta = 0.007$
Polyester	50 mm	$\sigma = 17049\ \mathrm{Ns/m^4}$
Microperforated Facing	0.3 mm	$d = 0.5\ \mathrm{mm}$ $p = 5.98\%$
Air Cavity	50 mm	$\rho_a = 1.25\ \mathrm{kg/m^3}$ $c = 343\ \mathrm{m/s}$

3. Results and Discussion

In the absence of flanking transmission, i.e., only Dd transmission path is considered in Fig. 1, the sound transmission loss of the numerical model with material and panel combinations shown in Table 1 is validated by an analytical formulation based on an infinite panel theory [21]. Fig. 3 shows this comparison in the frequency range of 10 Hz to 12,500 Hz. In the frequency range up to 250 Hz the analytical calculations show noticeable differences owing to the boundary conditions, or lack of thereof, for the infinite panel. In this frequency range, the transmission loss is largely contributed by the stiffness of the panel and resonant frequencies. This behaviour can be observed by the dips in the transmission loss at 24 Hz and 93 Hz for the steel case, where due to the bending modes of the plate the resonant transmission increases from the panel into the acoustic domain. At higher frequencies, the STL calculations are similar. Overall STL characteristics of all panel configurations show that porous inclusions and thermoviscous losses via micro perforations induce acoustic energy losses far greater than those achievable by the mass density law, especially at frequencies above the coincidence region.

In practice, it is difficult to isolate the STL performance of a panel (or partition) due to flanking transmission through air-borne or structure-borne paths, such as transmission through joints, sound leakage from cracks and openings, and, if poorly designed, from the test facility itself. Assuming that the thick concrete construction sufficiently blocks the noise coming from outside of the test rooms, also blocking the transmission across the rooms, and that the vibration isolators are installed on the floors in the construction of the facility, flanking transmission through the facility, i.e., Ff and Df in Fig. 1, will be negligible compared to other sources. The filler wall with a small test opening is constructed from heavyweight concrete or brick sections, and mineral wool is used to fill the gap in between. For thin panels or lightweight partitions, this type of filler wall can block out most of the flanking transmission. However, for multi-layer panels, such as the one in Fig. 2, there may occur flanking transmission due to joints (bolt connections), air leakage due to improper sealing of the outer layer, or vibration transmission from the filler wall radiating into the air cavity within the multi-layer panel thereby increasing the sound pressure measured on the receiving room.

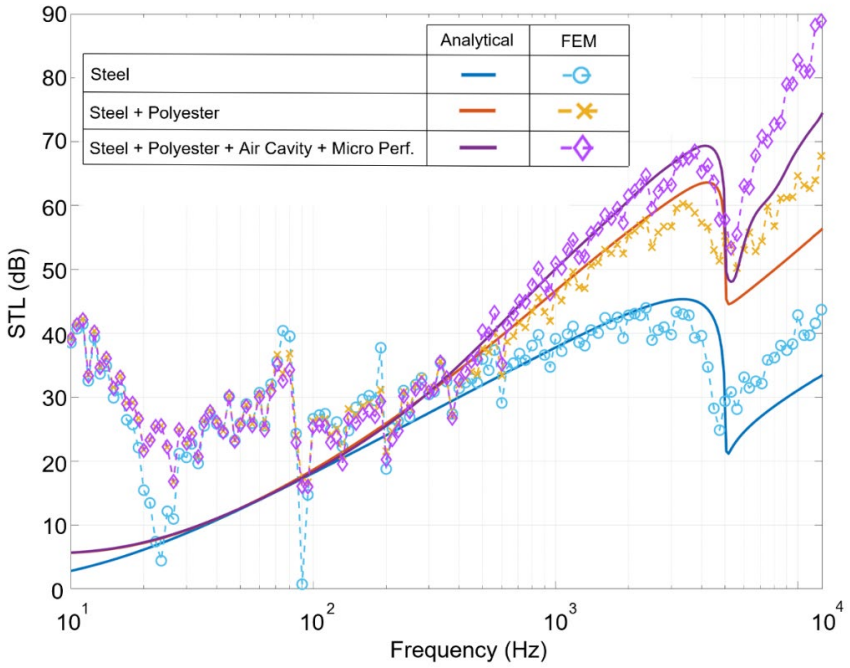

Figure 3: Comparison of analytical (infinite panel theory) and numerical (COMSOL Multiphysics) studies of sound transmission loss of a 1 m × 1 m panel with material combinations (Table 1).

In a numerical model possible flanking transmission sources and paths are implemented, such as the ones in Fig. 1, as a case study to investigate the amount and significance of the flanking transmission in STL measurement of a multi-layer panel. Point loads, shown by N1 to N5 in Fig. 2, denote the discrete dynamic loads on the panel due to clamping via bolt connections. If the number these joints increase across the perimeter of the panel, it can be assumed to have a uniform clamping on the panel which can also be approximated by a distributed (line) load. Fig. 4a shows a comparison of different clamping scenarios with respect to point and distributed line loads. Applying $F = 0.01$ N load through N1 bolt connection shifted the STL across the frequency measurement range, whereas this change was limited for additional bolt connections. It is observed that the increasing number of contact points for clamping force converges to a distributed load case. The greater the clamping force directly applied on the panel, the more effectively the panel radiates, as observed by the large shifts in STL for $F = 0.05$ N and 1 N in Fig. 4b, indicating that loose bolt connections or uneven clamping force can contribute to significant flanking transmission in an actual test.

Air-borne transmission through slits and cracks and structure-borne energy leaking through indirect transmission paths may also contribute to flanking transmission, as denoted by monopole point source and boundary load (wall transmission) representations in Fig. 2, respectively. Though the selection of the strength of these sources is arbitrary in this numerical study, it can be observed in Fig. 4c that these flanking transmission paths can be significant in the measurement of STL from a multi-layer panel; in particular, the monopole point source has shifted the STL by almost 10 dB around 1,200 Hz indicating that airborne transmission paths can be more dominant at high frequencies (Fig. 4c).

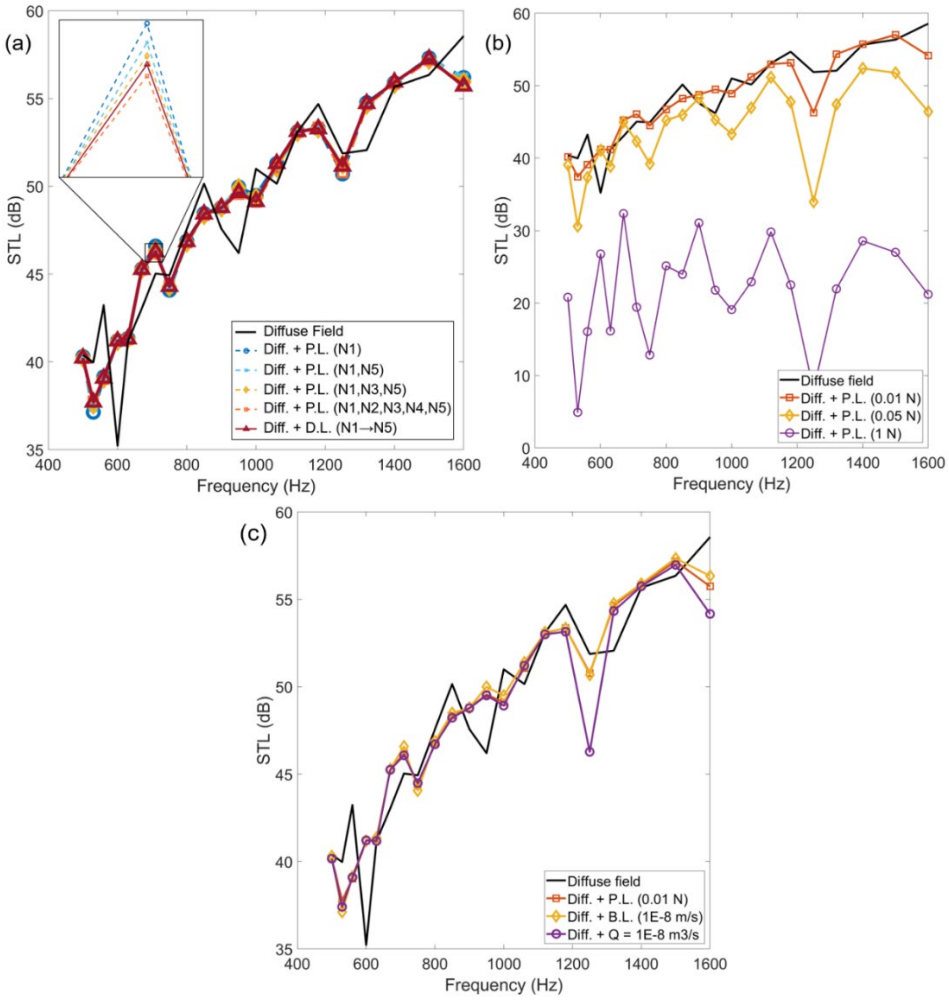

Figure 4: Investigation of the effect of point load (as approximation of clamping force) and flanking transmission sources on the STL. (a) Comparing different number of point loads (of 0.01 N) and a distributed loading case where N1 to N5 correspond to locations in Fig. 2; (b) Comparing the effect of the magnitude of point load on the STL for all edges clamped case; (c) Comparison of all three flanking transmission sources denoted in Fig. 2.

4. Conclusions

This paper has presented an initial numerical investigation into the quantification of flanking transmission in multilayer panels by considering structural and acoustic transmission paths. It has been demonstrated that point load of greater magnitude applied on the panel can reduce the STL performance significantly due to increasing the acoustic radiation from the panel. The boundary transmission and sound leakage may also induce considerable flanking transmission. Future work is needed to validate these findings experimentally and improve the design of the test wall currently under construction in order to obtain better STL predictions.

Acknowledgments

The authors acknowledge the support of the Defence Science and Technology Group.

REFERENCES

1 Buckingham, E. Theory and implementation of experiments on the transmission of sound through partition walls, *Sci. Papers Bur. Standards*, **20**, 193, (1925).
2 London, A. Tentative Recommended Practice for Laboratory Measurement of Airborne-Sound Transmission Loss of Building Floors and Walls, *The Journal of the Acoustical Society of America*, **23**, 686–689, (1951).
3 Beranek, L. L. The Transmission and Radiation of Acoustic Waves by Structures, *Proceedings of the Institution of Mechanical Engineers*, **173**, 12–35, (1959).
4 Bhattacharya, M. C., Guy, R. W., Crocker, M. J. Coincidence effect with sound waves in a finite plate, *Journal of Sound and Vibration*, **18**, 157–169, (1971).
5 Sewell, E. C. Transmission of reverberant sound through a single-leaf partition surrounded by an infinite rigid baffle, *Journal of Sound and Vibration*, **12**, 21–32, (1970).
6 Davy, J. L. The forced radiation efficiency of finite size flat panels that are excited by incident sound, *The Journal of the Acoustical Society of America*, **126**, 694–702, (2009).
7 Wareing, R. R., Davy, J. L., Pearse, J. R. Variations in measured sound transmission loss due to sample size and construction parameters, *Applied Acoustics*, **89**, 166–177, (2015).
8 Yao, D., Zhang, J., Wang, R., Xiao, X. Effects of mounting positions and boundary conditions on the sound transmission loss of panels in a niche, *J. Zhejiang Univ. Sci. A.*, **21**, 129–146 (2020).
9 Vinokur, R. Mechanism and calculation of the niche effect in airborne sound transmission, *The Journal of the Acoustical Society of America*, **119**, 2211–2219, (2006).
10 Halliwell, R. E., Warnock, A. C. C. Sound transmission loss: Comparison of conventional techniques with sound intensity techniques, *The Journal of the Acoustical Society of America*, **77**, 2094–2103, (1985).
11 Dijckmans, A., Vermeir, G. A Wave Based Model to Predict the Niche Effect on Sound Transmission Loss of Single and Double Walls, *Acta Acustica United with Acustica*, **98**, 111–119, (2012).
12 Mariner, T. Critique of the Reverberant Room Method of Measuring Air-Borne Sound Transmission Loss, *The Journal of the Acoustical Society of America*, **33**, 1131–1139, (1961).
13 ISO (International Organization for Standardization). *Acoustics-Laboratory Measurement of Sound Insulation of Building Elements–Part 3: Measurement of Impact Sound Insulation*, ISO 10140-3:2010, ISO, Geneva, Switzerland, (2010d).
14 ISO (International Organization for Standardization). *Acoustics-Laboratory Measurement of Sound Insulation of Building Elements–Part 4: Measurement Procedures and Requirements*, ISO 10140-4:2010, ISO, Geneva, Switzerland, (2010d).
15 Kuttruff, H. *Room acoustics*, 4th ed. Ed. Spon Press, London, [England]; New York, NY, (2000).
16 Kihlman, T., Nilsson, A. C. The effects of some laboratory designs and mounting conditions on reduction index measurements, *Journal of Sound and Vibration*, **24**, 349–364, (1972).
17 Kihlman, T. Sound transmission in building structures of concrete, *Journal of Sound and Vibration*, **11**, 435–445, (1970).
18 ISO (International Organization for Standardization). *Acoustics-Laboratory Measurement of Sound Insulation of Building Elements–Part 5: Requirements for Test Facilities and Equipment*, ISO 10140-5:2010, ISO, Geneva, Switzerland, (2010d).
19 Komatsu, T. Improvement of the Delany-Bazley and Miki models for fibrous sound-absorbing materials, A*coust. Sci. & Tech*., **29**, 121–129, (2008).
20 Atalla, N., Sgard, F. Modeling of perforated plates and screens using rigid frame porous models, *Journal of Sound and Vibration*, **303**, 195–208, (2007).
21 Dylejko, P. G., MacGillivray, I. R., Moore, S. M., Skvortsov, A. T. The influence of internal resonances from machinery mounts on radiated noise from ships, IEEE Journal of Ocean Engineering, 42(2), 399–409, (2016).